

# CloudBrain: Online neural computation in the cloud

Leon Bonde Larsen<sup>1,\*</sup>, Rasmus Karnøe Stagsted<sup>1</sup>, Beck Strohmer<sup>1</sup> and Anders Lyhne Christensen<sup>1</sup>

<sup>1</sup>SDU Biorobotics, Maersk McKinney Moller Institute, University of Southern Denmark

Correspondence\*:  
Leon Bonde Larsen  
lelar@mmmi.sdu.dk

## 1 ABSTRACT

2 Neuromorphic computing currently relies heavily on complicated hardware design to implement  
3 asynchronous, parallel and very large-scale brain simulations. This dependency slows down  
4 the migration of biological insights into technology. It typically takes several years from idea to  
5 finished hardware and once developed the hardware is not broadly available to the community. In  
6 this contribution, we present the CloudBrain research platform, an alternative based on modern  
7 cloud computing and event stream processing technology. Typical neuromorphic design goals,  
8 such as small form factor and low power consumption, are traded for 1) no constraints on the  
9 model elements, 2) access to all events and parameters during and after the simulation, 3) online  
10 reconfiguration of the network, and 4) real-time simulation. We explain principles for how neuron,  
11 synapse and network models can be implemented and we demonstrate that our implementation  
12 can be used to control a physical robot in real-time. CloudBrain is open source and can run on  
13 commodity hardware or in the cloud, thus providing the community a new platform with a different  
14 set of features supporting research into, for example, neuron models, structural plasticity and  
15 three-factor learning.

16 **Keywords:** Neuromorphic, Cloud, Robotics, Bio-inspired, Event-based, Stream-processing, Structural plasticity

## 1 INTRODUCTION

17 In traditional artificial neural networks (ANNs), the activation of neurons is represented as a scalar and  
18 information is propagated through the network in discrete steps. While this model can be computed  
19 efficiently on standard CPUs and GPUs, it is a very simplistic abstraction of biological neural networks.  
20 Biological neurons primarily communicate asynchronously through action potentials or *spikes* (Sterling  
21 and Laughlin, 2015). The timing of spikes can encode crucial information, for example in the auditory  
22 system where temporal information is used to infer direction of a sound source (Carr and Konishi, 1990;  
23 Haessig et al., 2020). Spiking neural networks (SNN) are a class of ANNs in which the temporal aspects of  
24 inter-neuron communication are explicitly considered: neurons asynchronously produce and communicate  
25 via discrete events (spikes), and SNNs thus allow encoding of information in the timing of the events.

26 Different spiking models have been described in literature ranging from the relatively simple integrate-and-  
27 fire model (Keat et al., 2001; Jolivet et al., 2004; Paninski et al., 2004) to the more complex Hodgkin-Huxley  
28 model (Hodgkin and Huxley, 1952). To improve biological fidelity there is, however, still a need for  
29 experimenting with new models. For example biological neurons can be non-spiking (Sterling and Laughlin,

30 2015) and there could be advantages of combining spiking and non-spiking models (Woźniak et al., 2020).  
31 Integrating non-spiking neurons in SNNs can be a biologically plausible way to interface analogue sensors  
32 and can provide more control over network behaviour (Strohmer et al., 2020).

33 Current implementations of learning, both in ANNs and SNNs, are based almost exclusively on adapting  
34 parameters in the synapses connecting the neurons. Such synaptic learning also plays a crucial role in  
35 biological learning, but in ensemble with for example structural adaptations of the network and influence  
36 from different neuromodulators providing reward signals or adapting neuron behaviour (Sterling and  
37 Laughlin, 2015; Price et al., 2017). In a neuromorphic engineering context, structural plasticity has been  
38 shown to improve facilitation of the hardware (Qi et al., 2018), increase success of learning a task in  
39 reinforcement learning (Spüler et al., 2015), and in unsupervised classification tasks (Roy and Basu,  
40 2017). Online adaptation of network structure is, however, not directly supported in current neuromorphic  
41 hardware, thus restricting research to pure simulations.

42 In this paper, we present the CloudBrain platform for simulating SNNs. CloudBrain utilises modern  
43 cloud technology to create an infrastructure capable of executing SNNs in a computer cluster. This gives  
44 several advantages: 1) There are practically no constraints on the model elements. If the concept can be  
45 described in code it will also run in the cluster. 2) It allows access to all events and parameters both online  
46 and offline, making it easier to monitor, develop and test solutions. 3) The structure of the network can be  
47 reconfigured online allowing model elements to affect connectivity. 4) The network can run online and  
48 control a robot through the *robot as a service* principle (Kuffner, 2010) to interact with the environment. 5)  
49 It runs on standard computers and is based on well-documented, field-tested, free, open source software.  
50 We present the architecture of CloudBrain, demonstrate the advantages of the approach, and deploy it in  
51 closed-loop control of a robot.

## 52 1.1 SNN simulators

53 SNNs can be simulated on PCs or supercomputers using specialised software such as the GENESYS  
54 (Bower et al., 2003) and NEURON (Carnevale and Hines, 2006) simulators or the more computationally  
55 tractable NEST (Gewaltig and Diesmann, 2007), BRIAN (Stimberg et al., 2019) and CARLsim (Chou  
56 et al., 2018). These simulators are very useful for investigating the behaviour of networks and of their  
57 constituent parts. Their limitation lies in not being able to embody the neural simulation for instance to  
58 control a physical robot. It has also been suggested that they are less suited for evolving models (Nowke  
59 et al., 2018) because the model requires external control while evolving.

60 An alternative to the software simulations is neuromorphic hardware. Since a spiking neuron only needs  
61 to do work whenever it receives a spike, it can operate asynchronously. That observation has been the  
62 basis for developing non-von-Neumann computer chips (Furber, 2016) leading to small, scalable, fast and  
63 energy-efficient devices for researching and deploying SNNs, such as SpiNNaker (Furber et al., 2014) and  
64 BrainScales (Schemmel et al., 2010) developed in the Human Brain Project, IBM's True North (Essera  
65 et al., 2016), Loihi from Intel (Davies et al., 2018), and the analog DYNAPs (Qiao et al., 2015; Moradi et al.,  
66 2018) developed at ETH Zurich. Such neuromorphic hardware is well suited for embodied experiments  
67 since the neuronal computations can run in real time, for example controlling a physical robot.

68 Each chip represents a trade-off between features and limitations. Common for all of them is that the  
69 interface to and from the chip is a bottleneck and does not allow the user to export all the spike events  
70 happening in the chip. This can complicate monitoring and makes it harder to analyse a network. The  
71 SpiNNaker platform (Furber et al., 2014) is available for loan but otherwise gaining access to neuromorphic  
72 hardware can be challenging because only few units exist or because intellectual property rights restrict its

73 use. Support in the form of software frameworks and documentation can also be limited as is support for  
74 special features, for example to investigate new neuron models.

75 More flexible hardware implementations of SNNs have been demonstrated on Field Programmable Gate  
76 Arrays (FPGAs) and Graphics Processing Units (GPUs). FPGAs are programmable devices consisting of  
77 numerous logic blocks that can be almost arbitrarily connected. Once programmed, the FPGA's performance  
78 is comparable to specialised chips. The use of FPGAs to simulate SNNs has been found to be highly  
79 scalable (Moore et al., 2012; Wang and van Schaik, 2018) and some work suggests vector processing  
80 implemented in FPGAs can help mitigate the memory bottleneck problem that reduces access to spikes and  
81 parameters (Naylor et al., 2013). However, the lack of hardware support for floating-point arithmetic limits  
82 FPGAs to the simpler neuron models and they do not easily support online changes to network structure.

83 FPGAs are still quite uncommon and programming them is very different from computer programming  
84 so their use requires special training. GPUs, on the other hand, are common in most modern PCs and  
85 implementations of SNNs on GPUs have been demonstrated to be highly scalable (Hoang et al., 2013;  
86 Chou et al., 2018). GeNN, a GPU-enhanced simulation software based on NVIDIA CUDA technology,  
87 even out-performed some state-of-the-art specialised chips with regards to speed and power-consumption  
88 (Knight and Nowotny, 2018). The availability of embedded GPU platforms, such as NVIDIA's Jetson TX2  
89 also enables GeNN to be used interactively to control a robot. The strong commercial development of  
90 GPUs is constantly moving the boundaries for what is possible but generally, moving data to and from the  
91 GPU memory is a bottleneck limiting access to spikes and parameters.

92 Sometimes hybrid systems can enable new features or remove limitations. For example the SpiNNaker  
93 million-core machine is available through the Human Brain Project's portal (Human Brain Project, 2017)  
94 for running even very large simulations and Intel Labs developed a cloud-based platform for research  
95 community access to scalable Loihi-based infrastructure (Intel, 2019). However, none of them support  
96 online experimentation, for example with robots. Brian2GeNN (Stimberg et al., 2020) is a software  
97 package that uses GeNN to accelerate simulations defined in Brian on GPU hardware. GPU acceleration of  
98 simulation software has also been demonstrated to improve performance on supercomputers and enable  
99 larger simulations on single computers (Hoang et al., 2013; Chou et al., 2018).

## 100 1.2 Cloud infrastructure

101 In recent years, cloud-based technology has seen rapid development driven by the demand for distributed  
102 and highly scalable IT-solutions (?). When executed in the cloud, a computer program often runs in a  
103 virtual environment called a *container*. Seen from the program the container is like any computer with  
104 resources such as CPU, memory, disk and an operating system while in fact the containers share these  
105 resources. Asynchronous, event-based architectures in particular have excelled in order to handle millions  
106 of social media users or e-commerce transactions. Programs are often asynchronous, meaning that they are  
107 waiting for input for example from a user requesting a website or completing a purchase. While waiting the  
108 program needs no computing resources and thus other programs in other containers can use the hardware.  
109 This fits well with the SNN model, where the neuron only does work when an input event is present.

110 Modern IT solutions generate a lot of data and it is common to handle it as event-streams (?). Event-  
111 streams are ordered in topics such that nodes subscribing to a topic receive events that are published  
112 on that topic. There can be many publishers and many subscribers to a topic and there can be many  
113 topics. Copying and distribution of the events are handled by highly optimised and extremely scalable  
114 infrastructure software making it easy to interface programs with the event-stream. Such an architecture is  
115 well suited for handling spike events since many neurons need to receive the same events.

## 2 ARCHITECTURE

116 An SNN simulation in CloudBrain is essentially a collection of small programs implementing mathematical  
117 models and communicating the resulting events as they happen. CloudBrain is the platform that runs the  
118 programs in a scalable and modular way. In CloudBrain, both neurons, synapses and any other models  
119 are user-defined programs, while spikes, parameters, and any other messages are events consisting of a  
120 timestamp and an arbitrary payload.

### 121 2.1 Programs

122 The *NeuronProgram* and *SynapsePrograms* run under the *ControlProgram* in order to hide the complexity  
123 of communication and OS-specific interfaces. One *ControlProgram* can run one *NeuronProgram* and  
124 multiple *SynapsePrograms* and to ensure scalability, the *ControlProgram* is executed in a container. Thus  
125 the *ControlProgram* can run on any host within the cluster and multiple *ControlPrograms* can run on the  
126 same host (figure 1). The user controls if the *ControlProgram* runs synchronously updating the neuron  
127 model at a specific rate or asynchronously only updating the model when a spike is received. The same  
128 goes for the *SynapseProgram* which is responsible for keeping information about the connections (for  
129 example weight and delay) and attaching it to the payload of received spikes before handing them to the  
130 *NeuronProgram*. The connection information is provided when the connection is first made but can also  
131 be updated during execution. *Events* are implemented as asynchronous messages transmitted following  
132 the publish-subscribe pattern (Birman and Joseph, 1987) so a *ControlProgram* receives messages only  
133 from topics it has subscribed to. Topics contain either *ControlEvents*, handled by the *ControlProgram*  
134 or *NeuroEvents*, passed first through a *SynapseProgram* and then handled by a *NeuronProgram*. Each  
135 *ControlProgram* has an individual *ControlTopic* that it always subscribes to while all other subscriptions  
136 are set up at run-time.

### 137 2.2 Global control

138 A *GlobalController* is responsible for scaling the number of containers in the cluster and for configuring  
139 the *ControlPrograms* by emitting *ControlEvents*. Each *ControlProgram* in the cluster has a unique ID  
140 known to itself and the *GlobalController*. To set up an experiment, the user writes a *GlobalController*  
141 program that tells each of the *ControlPrograms* which *NeuronProgram* and *SynapsePrograms* to run, which  
142 parameters to use and how to connect. It also defines any groupings of *NeuronPrograms*, for example  
143 into populations. If non-standard neuron models are used, they have to be implemented in code and either  
144 provisioned to the cluster before running the *GlobalController* or sent to the individual container using  
145 control events, during execution. The *GlobalController* can be run from any computer on the same network  
146 as the cluster.

### 147 2.3 Simulation method

148 Ideally, the *NeuronPrograms* and *SynapsePrograms* should be asynchronous, meaning that they only  
149 use processing resources when they receive or transmit an *Event*. This greatly improves performance but  
150 is not practical for all neuron models and thus they can also be periodic. To run asynchronously, every  
151 time a neuron receives a spike, it must predict when it will spike based on the mathematical model of the  
152 neuron and its internal parameters. The neuron then registers a timer to wake it at that time and removes  
153 any previously registered timers (figure 1).

154 Communication in the cluster is faster than in biological neurons. Because the *NeuronPrograms* calculate  
155 behaviour based on timestamps and not on the actual time of arrival, the cluster essentially spends the time

156 accounted for in the biological delays to complete the required calculations and communicate the results. If  
157 that time is insufficient, the post-synaptic neuron will know that a deadline was missed and can report it.  
158 The *SynapseProgram* receives incoming *SpikeEvents* and attaches the connection information (typically  
159 weight and delay) before passing them on to the *NeuronProgram*. When the *NeuronProgram* emits a spike,  
160 it also alerts the *SynapseProgram* thus allowing it to update the connection parameters according to its  
161 learning rule.

### 3 METHODS

162 A proof-of-concept implementation based on Python and open-source software was built in order to validate  
163 the proposed architecture. The code is available on a git repository along with a demo of CloudBrain  
164 running on a single PC and instructions on how to set up a cluster with a cloud provider. All is available at  
165 [sdu.dk/cloudbrain](https://sdu.dk/cloudbrain).

#### 166 3.1 Implementation

167 *ControlProgram* and *NeuronProgram* are written in Python. A custom *NeuronProgram* inherits from  
168 a base class so the user only needs to override the functions used and need not care about the inner  
169 workings of the *ControlProgram*. The functionality exposed by the *NeuronProgram* base class include  
170 methods to emit events and to register callback functions for event reception or the expiration of timers.  
171 The Python code is integrated in a minimalistic docker image (?) and executed in docker swarm (?). Using  
172 the continuous integration tools included in gitlab (?), the process of deploying the code on the docker  
173 swarm is automated. Log activity from the containers is collected using Filebeat (?), allowing the logs to  
174 be searched and viewed from a web-based interface. Events are handled by Apache Kafka (?), an open-  
175 source stream-processing software platform, providing high-throughput and low-latency communication.  
176 Messages are JSON encoded and consist of a timestamp, sender ID and an arbitrary payload. Since Kafka  
177 is agnostic to the payload, it can be seamlessly changed to fit any computational model, to set parameters in  
178 a *NeuronProgram* or to retrieve arbitrary information. One of the great advantages of an event-based system  
179 is the availability of tools to view, search and aggregate data. We use Elasticsearch and the visualisation  
180 dash-board Kibana. This allows for fast, online and virtually unconstrained visualisation of activity in the  
181 network, for example, to monitor spiking rates at population level or for individual neurons, to analyse  
182 behavioural patterns or to monitor the flow of *ControlEvents*.

#### 183 3.2 Hardware

184 The on-premises cluster consists of 15 PCs, each with 2 Intel Xeon 2.55GHz cores, 8 GB RAM, Gigabit  
185 network and with Debian9 installed on a solid state drive (figure 5 shows a photo of the cluster). An  
186 additional PC with Intel Xeon 2.67GHz quad-core, 12 GB RAM and SSD is used to run Kibana, Kafka,  
187 Elasticsearch connector and Zookeeper (used by kafka). Another PC with Intel I5 3.30 GHz quad-core, 12  
188 GB RAM and SSD is used to run Elasticsearch. Elasticsearch runs on a separate host to keep peak CPU  
189 and memory usage from interfering with the performance of Kafka. Finally a PC with Intel I5 2.90 GHz  
190 quad-core, 16 GB RAM and SSD was used to monitor the cluster using Grafana and InfluxDB. On each of  
191 the hosts in the cluster, Telegraf was installed to collect information about the utilisation of the nodes. The  
192 machines are connected to a gigabit managed switch using Cat5e cables and communication to the robot is  
193 provided by a VPN tunnel through a Wi-Fi access point. As an alternative to procuring an on-premises  
194 cluster, we repeated the experiments with Google Cloud Platform (GCP) executing CloudBrain. 14 virtual  
195 machines were configured each with 4 vCPUs running at 2 GHz, 15 GB RAM and 100GB disk. 10 VMs

196 were used to run the neurons and the rest were used as VPN gateway, Kafka broker, Elasticsearch and  
197 connectors to Elasticserch. All VMs were located in Finland while the robot was in Denmark.

### 198 **3.3 Robot platform**

199 The mobile robot described in Larsen et al. (2013) is optimised for rapid prototyping and consists of a  
200 wooden board with two rear wheels connected to motors and a castor wheel in front. In this work it was  
201 fitted with two custom bumper sensors, one on each side of the front (figure 5). An on-board RaspberryPi 3  
202 model B connected to the cluster via Wi-Fi is responsible for generating PWM signals for the motors based  
203 on received events and for emitting events based on the state of the sensors. A piece of software running in  
204 the cloud translates spikes into motor messages and sensor messages into spikes. An H-bridge supplies  
205 the current to the motors based on the generated PWM signals. The two sensors are implemented with  
206 micro-switches and each sensor emits spikes on its own topic. When the sensor is activated, it emits spikes  
207 with a frequency of 100Hz and when the sensor is not activated it emits spikes with a frequency of 10Hz.  
208 Each motor has its own topic and the output is controlled by a running average of the number of spikes  
209 received within the past 50ms. The average is then linearly mapped from 1-4 spikes to  $\pm 2$  wheel rotations  
210 per second, controlled by a standard PID controller.

211 During experiments the robot was enclosed in a 2.5m x 1.5m environment with slanted 25cm corners (see  
212 centre insert of figure 2). The environment can be configured as *corridor* or *box* by adding or removing the  
213 rectangle in the centre. The experiments were repeated several times in each configuration. The controller  
214 for the robot is based on the Braitenberg principle (Dennett and Braitenberg, 1986) where the left sensor has  
215 an inhibitory effect on the right motor and vice-versa. The network consists of six populations, each with  
216 five neurons (figure 2). Apart from the two sensor populations (A and B) and the two motor populations (C  
217 and D), an excitatory bias (E) is provided to both motor populations to make the robot move, and the last  
218 population (F) injects noise into the system to make the neurons fire out of phase.

### 219 **3.4 Neuronal models**

220 We implemented and tested three popular neuron models: Integrate-and-Fire (IF) (Keat et al., 2001;  
221 Jolivet et al., 2004; Paninski et al., 2004), Leaky-Integrate-and-Fire (LIF) (Stein, 1967; Tuckwell, 1989) and  
222 Adaptive-Exponential-Integrate-and-Fire (AEIF) (Brette and Gerstner, 2005; Gerstner and Brette, 2009).  
223 The IF and LIF neurons are implemented fully asynchronously so the neurons only use computational power  
224 when input spikes arrive or the neuron emits a spike. The AEIF model consists of two coupled differential  
225 equations that need to be integrated over time. To keep it asynchronous would make it computationally  
226 heavy because it would need to recalculate next spike time and set the timer accordingly every time a new  
227 spike arrives. Instead the model was implemented synchronously using the looping function with an update  
228 frequency of 1ms. We implemented the Spike-Timing-Dependent Plasticity (STDP) rule, such that it runs  
229 asynchronously and updates the weight of the synapse.

## 4 RESULTS

230 To support the claims that CloudBrain provides 1) no constraints on the model elements, 2) online  
231 reconfiguration of the network, 3) online operation, and 4) access to all information, we provide three  
232 demonstrations. We demonstrate 1) the implementations of three popular neuron models and a synapse  
233 model, 2) that the morphology of the network can be changed during operation, and 3) that a robot can be  
234 controlled online by CloudBrain running on a cluster. Furthermore, to demonstrate how all information in

235 the SNN can be monitored online, we provide the live plots from Kibana. Finally, we evaluate timing and  
236 load both on our own cluster and with a cloud provider.

#### 237 **4.1 Model implementations**

238 To demonstrate the implemented neuron models, two different experiments were made. In the first one,  
239 a spike source was connected to the IF and LIF, respectively and their voltage potential and firing was  
240 observed (figure 3, top). The voltage potential of the IF neuron increases linearly until it fires, whereas  
241 the voltage potential of the LIF neuron charges exponentially. The AEIF model was tested in the regular  
242 bursting mode with constant current input (Naud et al., 2008) using parameters from NEST (Gewaltig and  
243 Diesmann, 2007) while voltage potential, adaptation variable and spiking pattern were observed (figure 3,  
244 middle). The voltage potential of the AEIF neuron depends on the adaptation variable and, as it falls to a  
245 certain level, the neuron bursts. This confirms normal behaviour for all three neuron models.

246 Synaptic learning is demonstrated in a setup where a noisy spike source has excitatory connections to two  
247 LIF neurons. The two LIF neurons are connected with a synapse using STDP on all pre- and post synaptic  
248 events. The noisy spike source emits events with a random time difference between 100 ms and 1 s. Every  
249 time one of the LIF neurons spikes, the STDP synapse will update its weight based on the time since the  
250 other neuron last spiked. Figure 4 shows the evolution of synaptic weight in an STDP synapse. From the  
251 zoomed-in figure, we see that when a pre-synaptic spike occurs (green vertical line) the weight increases by  
252 an amount inversely proportional to the time since last post-synaptic spike. Similarly at the post-synaptic  
253 spike times the weight is reduced inversely proportional to the time since last pre-synaptic spike.

#### 254 **4.2 Morphology**

255 To demonstrate that the network can be reconfigured online, an experiment was made with a 10Hz spike  
256 source (A) and two IF neurons (B and C). After 5 seconds, the source is connected to neuron B thus making  
257 it fire. After another 10 seconds, the connection is removed and the same procedure is repeated for neuron  
258 C. We plot the spiking pattern of the three neurons in figure 3. The morphology changes shown here are  
259 very basic, but demonstrate that connections can be created, updated or removed by sending ControlEvents.

#### 260 **4.3 Online operation**

261 To demonstrate online operation, two experiments with the robot are reported, each in a different  
262 environment. The spiking rate of the populations were plotted online in Kibana and the resource use in the  
263 cluster were plotted using Grafana. Here we provide screenshots from both and a video of the experiment is  
264 available in the supplementary material. The experiments were run on the on-premises cluster and repeated  
265 in the GCP cluster.

266 To evaluate the total delay in the robot experiments, we used videos to analyse reaction times when the  
267 robot is colliding with the wall. We also estimated the delay from a change in spike rate of the sensor  
268 population until the corresponding change in the opposite motor population. This represents the total delay  
269 in the neuronal system without the robot. The delay of a single event through Kafka was measured by  
270 subscribing to a topic and publishing 100 events on it. This was measured both over WiFi and within the  
271 clusters. We report the median of the 100 measurements along with the 1st and 99th percentiles.

272 The robot was able to negotiate both corridor and box, reacting quickly and displaying the expected  
273 Braitenberg behaviour. The total delay from sensor activation to motor reaction was estimated based  
274 on several collisions with the wall, recorded on video. Upon collision the robot was thrown back a few  
275 centimetres and the controller reaction was fast enough to prevent the robot from hitting the wall again. It

276 took on average 5 frames (min. 4 frames, max. 8 frames), corresponding to 166 ms (min. 133 ms, max.  
277 266 ms) to react. There are different contributions to this delay, mainly the characteristics of the motor. The  
278 total delay from a change in a sensor population to the corresponding change in the motor population could  
279 not be determined precisely due to noise but was estimated to 30–80 ms based on the plots from Kibana  
280 (figure 5). The delay of a single event through Kafka was measured over 100 messages. The time from an  
281 event was sent until it was received was 24 ms via Wi-Fi (median: 24.0 ms, 1st: 8.0 ms, 99th: 320.4 ms)  
282 and 4.2 ms within the cluster (median: 4.2 ms, 1st: 2.7 ms, 99th: 5.5 ms).

283 Figure 5 also shows the load on the cluster while the robot is navigating the corridor. The memory usage  
284 is constant because once the neurons are running they do not make additional allocations. The network  
285 usage is less than 2%. For comparison, the idle cluster had memory usage of 6%, CPU usage 3% and  
286 network 0%. Under the experiment an average of 1930 spikes per second were passing through Kafka.  
287 Benchmarking of the Kafka broker showed that it could handle approximately 400.000 spikes per second.

288 The same experiment was conducted on GCP for a duration of 15 minutes. Similar to the delay measured  
289 with the on-premises cluster, the latency was measured from the robot to the GCP. The delay measured to  
290 47.3 ms (median: 46.7 ms, 1st: 46.2 ms, 99th: 52.6 ms). The spike delay within the cluster was measured  
291 to 3.5 ms (median: 3.2 ms, 1st: 2.7 ms, 99th: 5.5 ms).

292 The *ControlProgram* allows the user to toggle live logging of internal variables and parameters. The  
293 values are sent, as events, only when they change. The plots in figure 3 and 5 are all live screenshots  
294 from Kibana demonstrating that parameters are available online. Data can also be accessed online without  
295 Kibana for more advanced plots or extracted for offline generation of plots better suited for publication.

## 5 DISCUSSION AND CONCLUSION

296 In this contribution, we propose a novel architecture for simulating spiking neural networks on readily  
297 available cloud infrastructure. We describe a proof-of-concept implementation, demonstrating how neuron  
298 and synapse models can be implemented and how the network connections can be updated while the system  
299 is running. Finally we demonstrate how a Braitenberg-controlled differential drive robot could be operated  
300 online from both our on-premises cluster and from a Google Cloud Platform cluster.

301 The numbers provided are highly dependent on hardware, application and other implementation specific  
302 factors. We therefore provide the numbers observed in our proof-of-concept implementation without  
303 expecting them to generalise perfectly to other implementations. Our on-premises cluster built from 15  
304 refurbished PCs over ten years old was able to support the experiments in this paper and the total cost of  
305 running the robot experiment for 15 minutes on GCP was approximately 2 USD. This shows that hardware  
306 for this type of simulation is readily available.

307 We did experience some jitter in the delay times and occasionally an event was late by a factor of  
308 hundreds which means it missed the deadline and thus essentially was lost. In our applications it was not a  
309 problem but means of mitigation should be further investigated. The Kafka broker can handle approximately  
310 400,000 spikes per second and this number scales linearly with the number of brokers. There are no limits  
311 in principle to the size of a computer cluster and cloud providers put huge clusters at our disposal. We  
312 simulated networks with up to 30 neurons for this paper but much larger networks should be possible  
313 and will be the focus of further work. In conclusion, we demonstrated key features that make CloudBrain  
314 especially suited for some types of experiments and argue that trading small form factor and low power  
315 consumption for such extra features can be sensible for research purposes.



## 6 ACKNOWLEDGEMENTS

316 We thank Mathias Neerup for invaluable help setting up CloudBrain and for discussions on architecture  
317 and implementation. We thank Cao Danh Do and Emil Bonde Larsen for help preparing the robot and its  
318 environment. Finally we thank SDU-Biorobotics and The Centre for BioRobotics for funding the project.

## REFERENCES

- 319 Birman, K. and Joseph, T. (1987). Exploiting virtual synchrony in distributed systems. *ACM SIGOPS*  
320 *Operating Systems Review* 21, 123–138. doi:10.1145/37499.37515
- 321 Bower, J. M., Beeman, D., and Hucka, M. (2003). The GENESIS simulation system. *The Handbook of*  
322 *Brain Theory and Neural Networks*, 475–478
- 323 Brette, R. and Gerstner, W. (2005). Adaptive exponential integrate-and-fire model as an effective description  
324 of neuronal activity. *Journal of Neurophysiology* 94, 3637–3642. doi:10.1152/jn.00686.2005
- 325 Carnevale, N. T. and Hines, M. L. (2006). *The NEURON book*. doi:10.1017/CBO9780511541612
- 326 Carr, C. E. and Konishi, M. (1990). A circuit for detection of interaural time differences in the brain stem  
327 of the barn owl. *Journal of Neuroscience* 10, 3227–3246. doi:10.1523/jneurosci.10-10-03227.1990
- 328 Chou, T. S., Kashyap, H. J., Xing, J., Listopad, S., Rounds, E. L., Beyeler, M., et al. (2018). CARLsim 4:  
329 An Open Source Library for Large Scale, Biologically Detailed Spiking Neural Network Simulation  
330 using Heterogeneous Clusters. In *Proceedings of the International Joint Conference on Neural Networks*  
331 (Institute of Electrical and Electronics Engineers Inc.), vol. 2018-July. doi:10.1109/IJCNN.2018.  
332 8489326
- 333 Davies, M., Srinivasa, N., Lin, T.-H., Chinya, G., Cao, Y., Choday, S. H., et al. (2018). Loihi: A  
334 neuromorphic manycore processor with on-chip learning. *IEEE Micro* 38, 82–99
- 335 Dennett, D. C. and Braitenberg, V. (1986). Vehicles: Experiments in Synthetic Psychology. *The*  
336 *Philosophical Review* 95, 137. doi:10.2307/2185146
- 337 Essera, S. K., Merollaa, P. A., Arthura, J. V., Cassidy, A. S., Appuswamy, R., Andreopoulou, A., et al.  
338 (2016). Convolutional networks for fast energy-efficient neuromorphic computing. *Proc. Nat. Acad. Sci.*  
339 *USA* 113, 11441–11446
- 340 [Dataset] Furber, S. (2016). Large-scale neuromorphic computing systems. doi:10.1088/1741-2560/13/5/  
341 051001
- 342 Furber, S. B., Galluppi, F., Temple, S., and Plana, L. A. (2014). The SpiNNaker project. *IEEE. Proceedings*  
343 102, 652–665. doi:10.1109/JPROC.2014.2304638
- 344 Gerstner, W. and Brette, R. (2009). Adaptive exponential integrate-and-fire model. *Scholarpedia* 4, 8427.  
345 doi:10.4249/scholarpedia.8427
- 346 Gewaltig, M.-O. and Diesmann, M. (2007). NEST (NEural Simulation Tool). *Scholarpedia* 2, 1430.  
347 doi:10.4249/scholarpedia.1430
- 348 Haessig, G., Milde, M., Aceituno, P. V., Oubari, O., Knight, J. C., van Schaik, A., et al. (2020). Event-based  
349 computation for touch localization based on precise spike timing. *Frontiers in Neuroscience* 14, 1–29.  
350 doi:10.3389/fnins.2020.00420
- 351 Hoang, R. V., Tanna, D., Jayet Bray, L. C., Dascalu, S. M., and Harris, F. C. (2013). A novel  
352 CPU/GPU simulation environment for large-scale biologically realistic neural modeling. *Frontiers in*  
353 *Neuroinformatics* 7, 19. doi:10.3389/fninf.2013.00019
- 354 Hodgkin, A. L. and Huxley, A. F. (1952). A quantitative description of membrane current and its application  
355 to conduction and excitation in nerve. *The Journal of Physiology* 117, 500–544. doi:10.1113/jphysiol.  
356 1952.sp004764

- 357 [Dataset] Human Brain Project (2017). Silicon Brains  
358 [Dataset] Intel (2019). Beyond Today's AI
- 359 Jolivet, R., Lewis, T. J., and Gerstner, W. (2004). Generalized integrate-and-fire models of neuronal activity  
360 approximate spike trains of a detailed model to a high degree of accuracy. *Journal of Neurophysiology*  
361 92, 959–976. doi:10.1152/jn.00190.2004
- 362 Keat, J., Reinagel, P., Reid, R. C., and Meister, M. (2001). Predicting every spike: A model for the  
363 responses of visual neurons. *Neuron* 30, 803–817. doi:10.1016/S0896-6273(01)00322-1
- 364 Knight, J. C. and Nowotny, T. (2018). GPUs Outperform Current HPC and Neuromorphic Solutions  
365 in Terms of Speed and Energy When Simulating a Highly-Connected Cortical Model. *Frontiers in*  
366 *Neuroscience* 12, 941. doi:10.3389/fnins.2018.00941
- 367 Kuffner, J. (2010). Cloud-enabled robots In: IEEE-RAS international conference on humanoid robots.  
368 *Piscataway, NJ: IEEE*
- 369 Larsen, L. B., Olsen, K. S., Ahrenkiel, L., and Jensen, K. (2013). Extracurricular Activities Targeted  
370 towards Increasing the Number of Engineers Working in the Field of Precision Agriculture . XXXV  
371 *CIOSTA & CIGR V Conference* , 1–12
- 372 Moore, S. W., Fox, P. J., Marsh, S. J., Markettos, A. T., and Mujumdar, A. (2012). Bluehive - A field-  
373 programable custom computing machine for extreme-scale real-time neural network simulation. In  
374 *Proceedings of the 2012 IEEE 20th International Symposium on Field-Programmable Custom Computing*  
375 *Machines, FCCM 2012*. 133–140. doi:10.1109/FCCM.2012.32
- 376 Moradi, S., Qiao, N., Stefanini, F., and Indiveri, G. (2018). A Scalable Multicore Architecture with  
377 Heterogeneous Memory Structures for Dynamic Neuromorphic Asynchronous Processors (DYNAPs).  
378 *IEEE Transactions on Biomedical Circuits and Systems* 12, 106–122. doi:10.1109/TBCAS.2017.  
379 2759700
- 380 Naud, R., Marcille, N., Clopath, C., and Gerstner, W. (2008). Firing patterns in the adaptive exponential  
381 integrate-and-fire model. *Biological Cybernetics* 99, 335–347. doi:10.1007/s00422-008-0264-7
- 382 Naylor, M., Fox, P. J., Markettos, A. T., and Moore, S. W. (2013). Managing the FPGA memory wall:  
383 Custom computing or vector processing? In *2013 23rd International Conference on Field Programmable*  
384 *Logic and Applications, FPL 2013 - Proceedings* (IEEE Computer Society). doi:10.1109/FPL.2013.  
385 6645538
- 386 Nowke, C., Diaz-Pier, S., Weyers, B., Hentschel, B., Morrison, A., Kuhlen, T. W., et al. (2018). Toward  
387 rigorous parameterization of underconstrained neural network models through interactive visualization  
388 and steering of connectivity generation. *Frontiers in Neuroinformatics* 12, 32. doi:10.3389/fninf.2018.  
389 00032
- 390 [Dataset] Paninski, L., Pillow, J. W., and Simoncelli, E. P. (2004). Maximum likelihood estimation of a  
391 stochastic integrate-and-fire neural encoding model. doi:10.1162/0899766042321797
- 392 Price, D. J., Jarman, A. P., Mason, J. O., and Kind, P. C. (2017). *Building brains - An introduction to*  
393 *neural development*. doi:10.1002/9781119293897
- 394 Qi, Y., Shen, J., Wang, Y., Tang, H., Yu, H., Wu, Z., et al. (2018). Jointly learning network connections  
395 and link weights in spiking neural networks. In *IJCAI International Joint Conference on Artificial*  
396 *Intelligence*. vol. 2018-July, 1597–1603. doi:10.24963/ijcai.2018/221
- 397 Qiao, N., Mostafa, H., Corradi, F., Osswald, M., Stefanini, F., Sumislawska, D., et al. (2015). A  
398 reconfigurable on-line learning spiking neuromorphic processor comprising 256 neurons and 128K  
399 synapses. *Frontiers in Neuroscience* 9. doi:10.3389/fnins.2015.00141

- 400 Roy, S. and Basu, A. (2017). An online unsupervised structural plasticity algorithm for spiking neural  
401 networks. *IEEE Transactions on Neural Networks and Learning Systems* 28, 900–910. doi:10.1109/  
402 TNNLS.2016.2582517
- 403 Schemmel, J., Briiderle, D., Gribbl, A., Hock, M., Meier, K., and Millner, S. (2010). A wafer-  
404 scale neuromorphic hardware system for large-scale neural modeling. In *Proceedings of 2010 IEEE*  
405 *International Symposium on Circuits and Systems* (IEEE), 1947–1950
- 406 Spüler, M., Nagel, S., and Rosenstiel, W. (2015). A spiking neuronal model learning a motor control task  
407 by reinforcement learning and structural synaptic plasticity. In *Proceedings of the International Joint*  
408 *Conference on Neural Networks*. vol. 2015-Sept. doi:10.1109/IJCNN.2015.7280521
- 409 Stein, R. B. (1967). Some Models of Neuronal Variability. *Biophysical Journal* 7, 37–68. doi:10.1016/  
410 S0006-3495(67)86574-3
- 411 Sterling, P. and Laughlin, S. (2015). *Principles of neural design*. doi:10.7551/mitpress/9780262028707.  
412 001.0001
- 413 Stimberg, M., Brette, R., and Goodman, D. F. (2019). Brian 2, an intuitive and efficient neural simulator.  
414 *eLife* 8. doi:10.7554/eLife.47314
- 415 Stimberg, M., Goodman, D. F., and Nowotny, T. (2020). Brian2GeNN: accelerating spiking neural network  
416 simulations with graphics hardware. *Scientific Reports* 10, 1–12. doi:10.1038/s41598-019-54957-7
- 417 Strohmer, B., Manoonpong, P., and Larsen, L. B. (2020). Integrating Non-Spiking Interneurons in Spiking  
418 Neural Networks. *bioRxiv*, 2020.08.13.249375doi:10.1101/2020.08.13.249375
- 419 Tuckwell, H. (1989). Introduction to theoretical neurobiology volume 2, nonlinear and stochastic theories.  
420 *Comparative Biochemistry and Physiology Part A: Physiology* 92, 268. doi:10.1016/0300-9629(89)  
421 90177-1
- 422 Wang, R. and van Schaik, A. (2018). Breaking Liebig’s law: An advanced multipurpose neuromorphic  
423 engine. *Frontiers in Neuroscience* 12, 593. doi:10.3389/fnins.2018.00593
- 424 Woźniak, S., Pantazi, A., Bohnstingl, T., and Eleftheriou, E. (2020). Deep learning incorporating  
425 biologically inspired neural dynamics and in-memory computing. *Nature Machine Intelligence* 2,  
426 325–336. doi:10.1038/s42256-020-0187-0

## FIGURE CAPTIONS

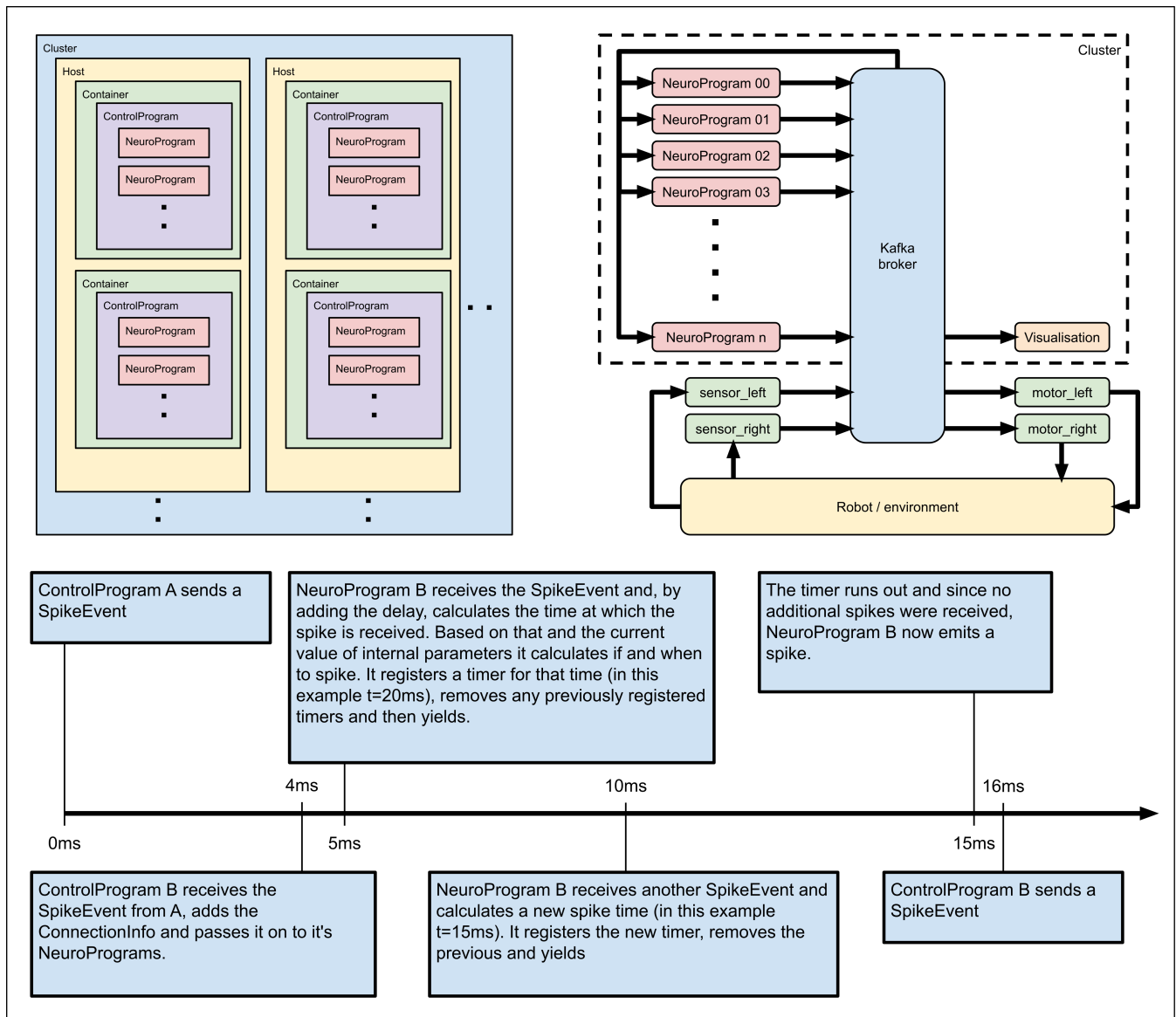


**Figure 1. Top left:** Shows how CloudBrain scales. Several *NeuroPrograms* can run under one *ControlProgram*. Several containers, each running one *ControlProgram*, can run on one host and the cluster is made up of any number of hosts. **Top right:** Conceptual overview of the robot experiment. The *NeuroPrograms* communicate through the kafka broker with the sensor and motor populations on the robot. **Bottom:** Simplified scenario demonstrating how asynchronous neuron models are implemented in CloudBrain.

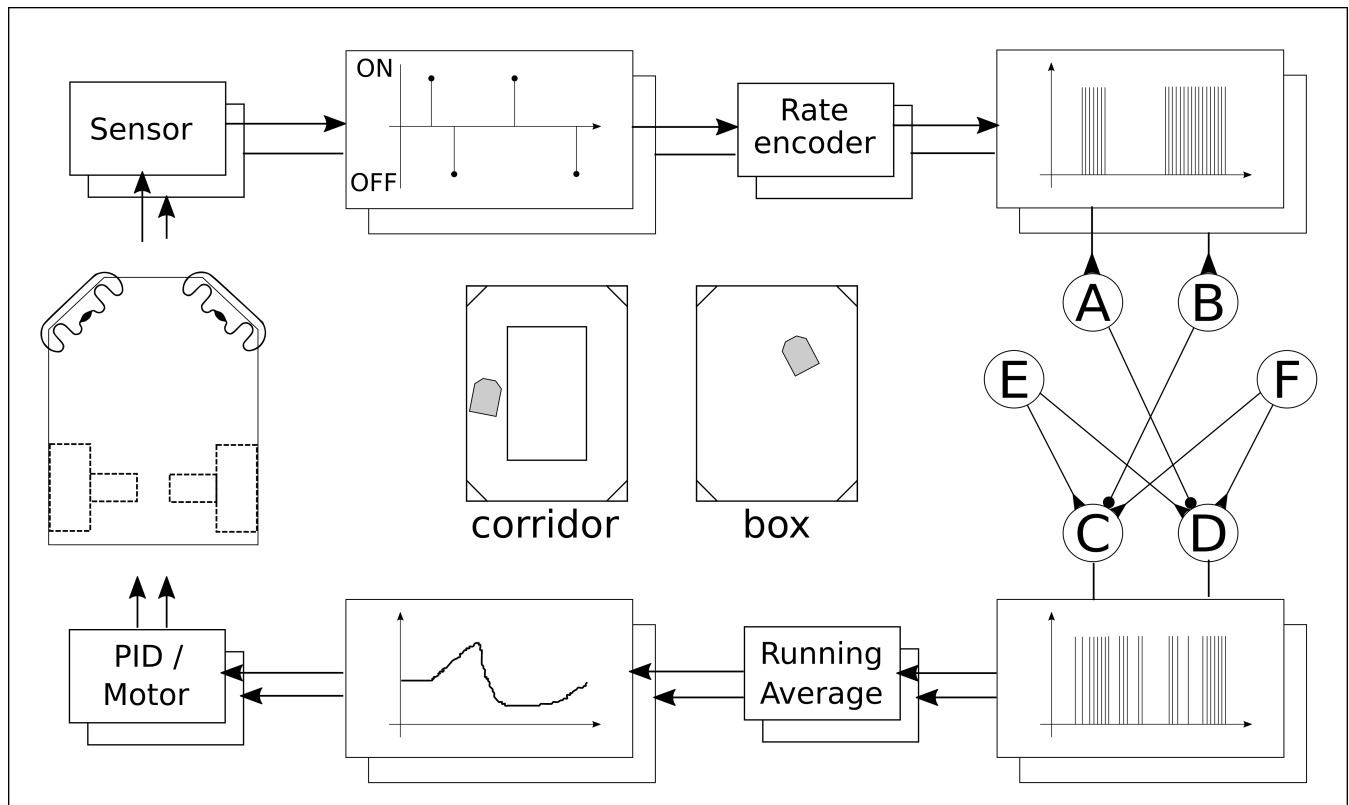


**Figure 2.** The control loop of the robot. Onset/offset events from the sensors are rate encoded and fed into populations A and B, respectively. E is injecting a bias (to keep the robot moving) and F injects noise. The motor neuron populations C and D are decoded by a running average and used as set-point in the PID for the motors. The centre insert shows the corridor track and the box track used for testing the robot.

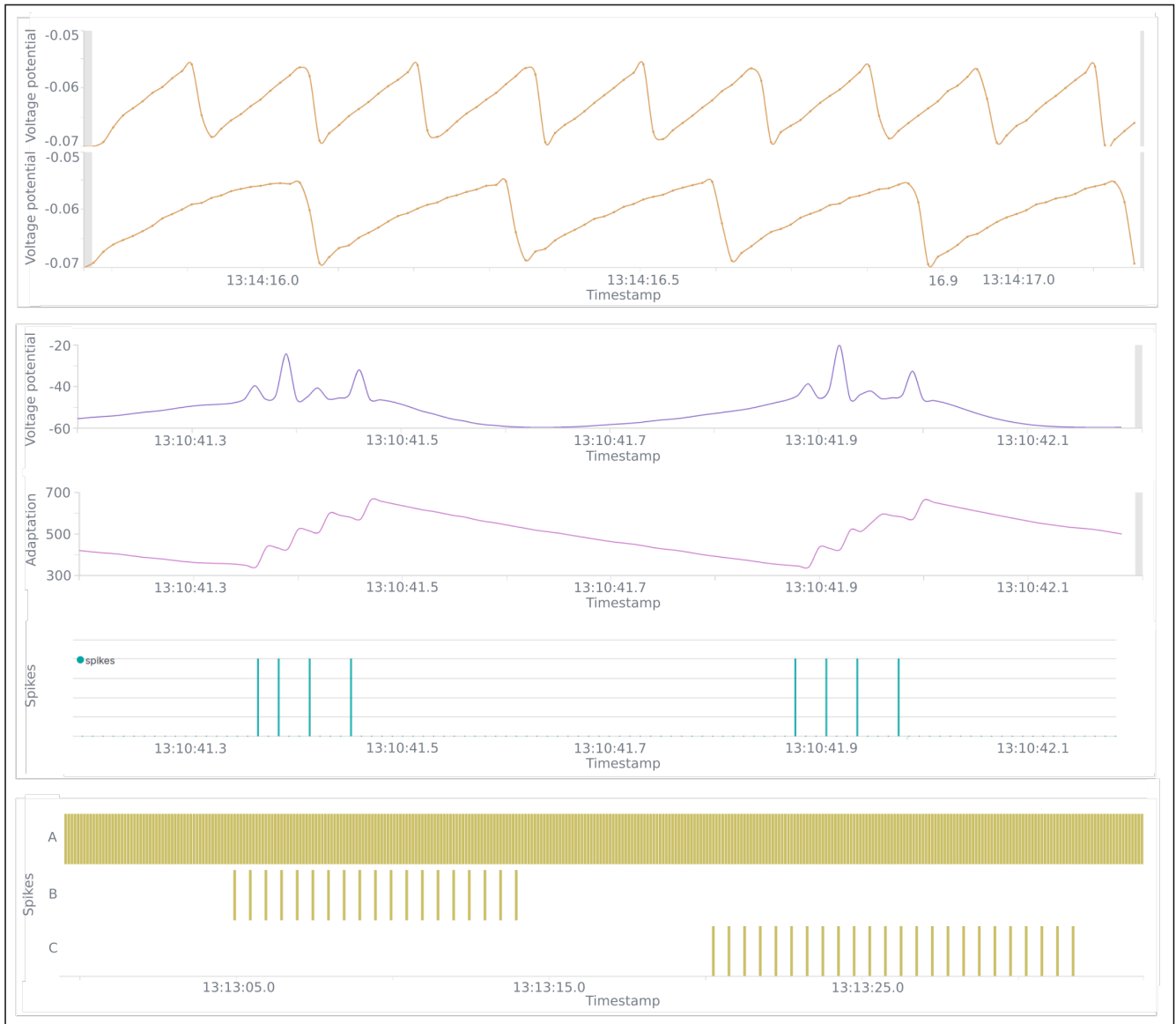


**Figure 3.** Screenshots from live monitoring in Kibana. **Top:** Voltage potential from experiment with Integrate-and-fire and Leaky-integrate-and-fire. **Middle:** Voltage potential, adaptation variable and spikes from experiment with Adaptive-exponential-integrate-and-fire. **Bottom:** Spikes from morphology experiment showing spikes from the spike source (top line) and from the two Integrate-and-fire neurons. The spike source is in turn connected to and disconnected from the neurons, causing them to spike.

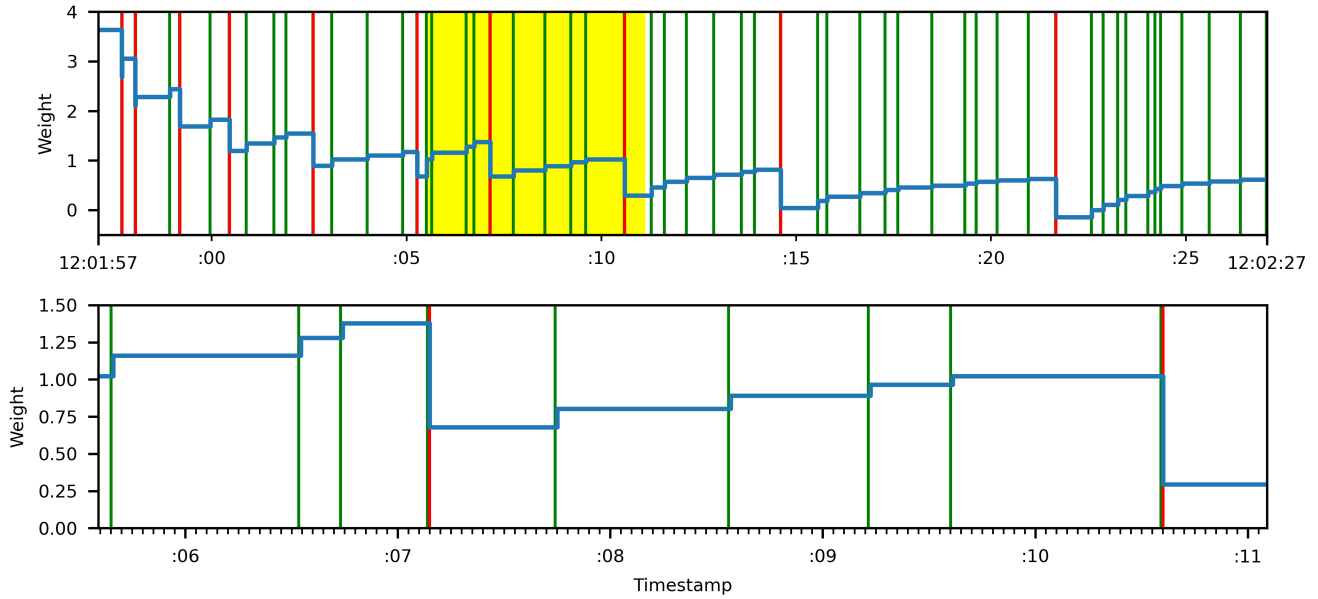


**Figure 4.** Synapse learning using STDP. Green vertical bars represent pre-synaptic spikes, while red vertical bars represent post-synaptic spikes. The blue line represents the synaptic weight. The bottom plot is a magnification of the yellow area in the top plot.

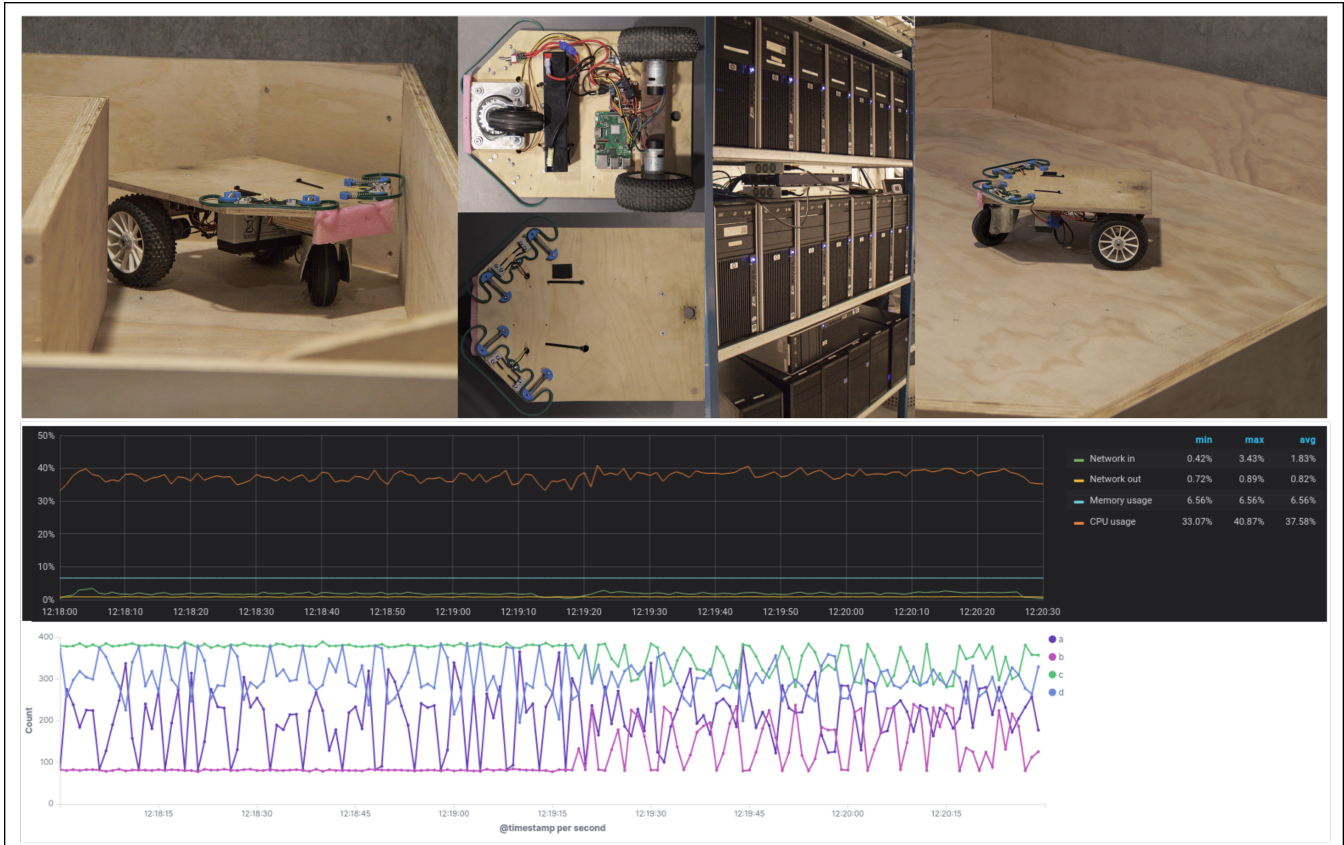


**Figure 5.** **Left image:** The robot in the corridor. **Right image:** The robot in the box. **Middle images:** The robot seen from below, the robot seen from above and the on-premise cluster. **Top plot:** Load on the cluster during operation. All values are taken as the percentage of the cluster’s total capacity. The plot is taken directly from Grafana as displayed live. **Bottom plot:** Spike rates on the interface populations (a/b for left/right sensor and c/d for left/right motor). The first half is in the box and the second half is in the corridor. While driving in the box, the robot displays a wall following behaviour thus always activating the same sensor and reacting with the same motor. The plot is taken directly from Kibana as displayed live.